Bioorganic Chemistry 105 (2020) 104362

Contents lists available at ScienceDirect

Bioorganic Chemistry

journal homepage: www.elsevier.com/locate/bioorg

Design, synthesis and biological evaluation of novel 1,3,4-thiadiazole derivatives as anti-glioblastoma agents targeting the AKT pathway

Monika Szeliga [a,*], Monika Karpińska [b], Radosław Rola [c], Andrzej Niewiadomy [b]

[a] Department of Neurotoxicology, Mossakowski Medical Research Centre, Polish Academy of Sciences, 5 Pawinskiego Str, 02-106 Warsaw, Poland
[b] Łukasiewicz Research Network – Institute of Industrial Organic Chemistry, 6 Annopol Str., 03-236 Warsaw, Poland
[c] Department of Neurosurgery and Paediatric Neurosurgery of the Lublin Medical University, 8 Jaczewskiego Str, 20-090 Lublin, Poland

ARTICLE INFO

Keywords:
Glioblastoma
Anti-glioblastoma compound
Thiadiazole derivative
Viability
Proliferation
AKT pathway

ABSTRACT

In spite of progress in understanding biology of glioblastoma (GBM), this tumor remains incurable with a median survival rate of 15 months. Previous studies have shown that 2-(4-fluorophenyloamino)-5-(2,4-dihydroxyphenyl)-1,3,4-thiadiazole (FPDT) and 2-(3-chlorophenyloamino)-5-(2,4-dihydroxyphenyl)-1,3,4-thiadiazole (CPDT) diminished viability of cancer cell lines of different origin. In the current study, we have examined activity of these compounds in several GBM cell lines and patient-derived GBM cells. We have also designed, synthesized and evaluated anti-GBM activity of novel 1,3,4-thiadiazole derivatives containing additional —Cl or $—CH_2CH_3$ substitute at C5-position of 2,4-dihydroxyphenyl. The tested compounds presented a considerable cytotoxicity against all GBM cell lines examined as well as patient-derived GBM cells. They were 15–110 times more potent than temozolomide, the first-line chemotherapeutic agent for GBM. Notably, in anticancer concentrations three of the derivatives were not toxic to human astrocytes. FPDT appeared to be the most promising compound with IC_{50} values between 45 μM and 68 μM for GBM cells and >100 μM for astrocytes. It augmented activity of temozolomide and inhibited proliferation migration and invasion of GBM cells. Treatment with FPDT diminished phosphorylation level of GSK3β and AKT. Pretreatment with PDGF-BB, an AKT activator, partially protected cells from death caused by FPDT, indicating that FPDT-mediated decrease in cell viability is causatively related to the inhibition of the AKT pathway.

1. Introduction

Glioblastoma (GBM, WHO IV) is the most frequent malignant primary brain tumor in adults. The standard of care for newly diagnosed GBM is maximal safe surgical resection, radiotherapy and concomitant and adjuvant chemotherapy with alkylating agent temozolomide (TMZ) (Fig. 1A) [1]. Despite the progress in understanding of biology of gliomagenesis made during the past decade, the clinical outcome of patients with GBM remains still poor: median survival time is approximately one year [2]. Diffuse growth and as well as inter- and intratumor heterogeneity are the most important hallmarks of GBM, which significantly contribute to therapeutic failure [3]. Moreover, the blood-brain barrier (BBB) and blood-tumor barrier (BTB) represent major obstacles to effective drug delivery [4]. Furthermore, side effects of each treatment cause significant decrease in quality of life. Therefore, continuous efforts should be made to find new molecular targets and effective therapies of GBM.

Abbreviations: ATCC, American Type Culture Collection; BBB, blood-brain barrier; BrdU, bromodeoxyuridine; BTB, blood-tumor barrier; CPCDT, 2-(3-chlorophenylamino)-5-(5-chloro-2,4-dihydroxyphenyl)-1,3,4-thiadiazole; CPDT, 2-(3-chlorophenyloamino)-5-(2,4-dihydroxyphenyl)-1,3,4-thiadiazole; CPEDT, 2-(3-chlorophenylamino)-5-(5-ethyl-2,4-dihydroxyphenyl)-1,3,4-thiadiazole; DMEM, Dulbecco's Modified Eagle's Medium; DMSO, dimethyl sulfoxide; EMEM, Eagle's Minimum Essential Medium Eagle; FBS, fetal bovine serum; FCS, fetal calf serum; FPCDT, 2-(4-fluorophenylamino)-5-(5-chloro-2,4-dihydroxyphenyl)-1,3,4-thiadiazole; FPDT, 2-(4-fluorophenyloamino)-5-(2,4-dihydroxyphenyl)-1,3,4-thiadiazole; FPEDT, 2-(4-Fluorophenylamino)-5-(5-ethyl-2,4-dihydroxyphenyl)-1,3,4-thiadiazole; GBM, glioblastoma; HA, human astrocytes; MTT, 3-(4,5-dimethylthiazol-2-yl)-2,5-diphenyl tetrazolium bromide; 2-(3-chlorophenyloamino)-5-(2, 4-dihydroxyphenyl)-1,3,4-thiadiazole; PBS, phosphate buffer saline; PDGF-BB, platelet-derived growth factor-BB; SClTB, sulfinylbis(5-chloro-2,4-dihydroxythiobenzoyl); SETB, sulfinylbis((5-ethyl-2,4-dihydroxyphenyl)methanethione); STB, sulfinylbis(2,4-dihydroxythiobenzoyl); TMZ, temozolomide.

* Corresponding author.
E-mail addresses: mszeliga@imdik.pan.pl (M. Szeliga), monika_karpinska2@wp.pl (M. Karpińska), rola.radoslaw@gmail.com (R. Rola), andrzej.niewiadomy@up.lublin.pl (A. Niewiadomy).

https://doi.org/10.1016/j.bioorg.2020.104362
Received 13 July 2020; Received in revised form 3 September 2020; Accepted 6 October 2020
Available online 9 October 2020

A

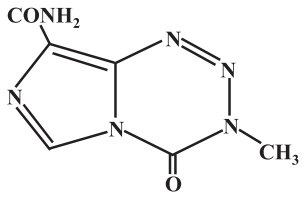

3-methyl-4-oxoimidazo[5,1-d][1,2,3,5]tetrazine-8-carboxamide
(temozolomide)

B

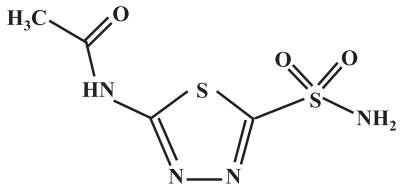

N-(5-sulfamoyl-1,3,4-thiadiazol-2-yl)acetamide
(acetazolamide)

C

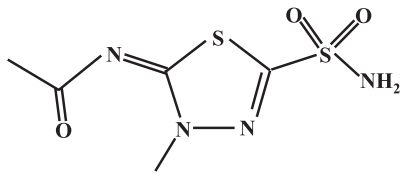

N-(3-Methyl-5-sulfamoyl-3H-1,3,4-thiadiazol-2-ylidene) ethanamide
(methazolamide)

Fig. 1. Chemical structure of the first-line chemotherapeutic for GBM, temozolomide (A) and two thiadiazole based clinically used drugs, acetazolamide (B) and methazolamide (C).

Thiadiazoles occurrs in nature in four isomeric forms 1,2,3-thiadiazole; 1,2,4-thiadiazole; 1,2,5-thiadiazole and 1,3,4,-thiadiazole. They exhibit a wide variety of biological activities, including antimicrobial, antifungal, antiviral, anti-inflammatory or anticonvulsant properties and increasing number of thiadiazole based drugs are currently available in the market [5]. Antineoplastic activity of different thiadiazole derivatives has been documented in a wide range of tumor cell lines [6–10] and *in vivo* [11,12]. The molecular mechanism underlying this activity most likely depends on the type of modification of thiadiazole ring. N-(5-sulfamoyl-1,3,4-thiadiazol-2-yl)acetamide (acetazolamide) (Fig. 1B) and N-(3-Methyl-5-sulfamoyl-3H-1,3,4-thiadiazol-2-ylidene) ethanamide (methazolamide) (Fig. 1C) are clinically used inhibitors of carbonic anhydrase [13]. Bis-2-(5 phenylacetamido-1,3,4-thiadiazol-2-yl) ethyl sulfide (BPTES) is an allosteric inhibitor of kidney type glutaminase isoform C [14], and similar mode of action was ascribed to a series of BPTES analogs [11,15,16]. A very recent study showed that 5-(3,5-dinitrophenyl)-1,3,4-thiadiazole derivatives incorporated with different heterocyclic systems inhibits activity of dihydrofolate reductase [17].

Two thiadiazole derivatives: 2-(4-fluorophenyloamino)-5-(2,4-dihydroxyphenyl)-1,3,4-thiadiazole (FPDT) and 2-(3-chlorophenyloamino)-5-(2,4-dihydroxyphenyl)-1,3,4-thiadiazole (CPDT) presented antiproliferative activity in several tumor cell lines derived from cancers of different origins including rat glioma C6 cell line, but had no influence on the viability of normal rat astrocytes and neurons [18,19]. The aim of the present study was to evaluate the efficacy of FPDT and CPDT in human GBM cell lines and cells isolated from human GBM tissues. The key premise is that potential anti-glioma drug should display antiproliferative activity in tumor cells without affecting normal tissues, therefore we also examined the influence of FPDT and CPDT on normal human primary astrocytes (HA). Moreover, the analysis was extended to four 1,3,4,-thiadiazole derivatives not tested so far. The newly tested compounds contain additional —Cl or —CH_2CH_3 substitute at C5-position of 2,4-dihydroxyphenyl. The choice of these modifications was guided by the literature data indicating that the hydrophobic substituent ($\pi > 0$) in the resorcinol ring can improve antiproliferative potency against cancer cells. It has been reported that the presence of a chlorine atom or ethyl (methyl, isopropyl) substituents in position 5 of resorcinol moiety of resorcylazoles can enhance their anticancer properties [20–22]. This finding was confirmed in the groups of 1H-benzimidazoles, 1,3-thiazolo[5,4-*b*]pyridines and 4H-3,1-benzothiazines substituted with 2,4-dihydroxyphenyl substituent [23–25]. Herein, both FPDT and CPDT notably decreased survival of GBM cells and FPDT did not display cytotoxic activity against non-transformed HA. The addition of either —Cl or —CH_2CH_3 substituent enhanced anti-GBM properties of the tested derivatives, but also significantly enhanced their toxic effects on HA. Hence, FPDT was subsequently subjected to further analysis to gain insight into possible biological mechanism of this compound.

2. Materials and methods

2.1. Synthesis of thiadiazole derivatives

The synthesis procedure of CPDT and FPDT was described previously [26]. Four other thiadiazole derivatives analyzed in this study were: 2-(4-Fluorophenylamino)-5-(5-chloro-2,4-dihydroxyphenyl)-1,3,4-thiadiazole (FPCDT); 2-(4-Fluorophenylamino)-5-(5-ethyl-2,4-dihydroxyphenyl)-1,3,4-thiadiazole (FPEDT); 2-(3-Chlorophenylamino)-5-(5-chloro-2,4-dihydroxyphenyl)-1,3,4-thiadiazole (CPCDT); 2-(3-Chlorophenylamino)-5-(5-ethyl-2,4-dihydroxyphenyl)-1,3,4-thiadiazole (CPEDT). The chemical structures of the tested compounds are depicted in Fig. 2.

All derivatives were prepared by the reaction of sulfinylbis(2,4-dihydroxythiobenzoyl) (STB), sulfinylbis(5-chloro-2,4-dihydroxythi obenzoyl) (SClTB) or sulfinylbis((5-ethyl-2,4-dihydroxyphenyl)meth anethione) (SETB) with commercially available thiosemicarbazides in the endocyclization reaction. Briefly, STB, SClTB or SETB was mixed with either 4-(4-fluorophenyl)-3-thiosemicarbazide or 4-(3-chlorophenyl)-3-thiosemicarbazide (Alfa Aesar) in methanol and refluxed for 3 h. The reaction mixture was hot filtered and the product was crystallized from methanol. Subsequently, the compounds were subjected to in-depth analytical studies. The results of these analyses are following:

2-(4-Fluorophenylamino)-5-(2,4-dihydroxyphenyl)-1,3,4-thiadiazole (FPDT): Yield: 69%, mp: 279–280 °C. EI-MS (*m/z*, %): 303 (M+, 100), 168 (39), 135 (11), 136 (14), 121 (4), 109 (3), 110 (8), 95 (5), 94 (12), 83 (6), 66 (6). 1H NMR (500 MHz, DMSO-d_6, δ): 10,85 (s, 1H, *C*2-OH), 10,27 (s, 1H, C4-OH), 9,92 (s, 1H, NH), 7,82–7,84 (d, 1H, C6-H), 7,61–7,70 (m, 2H, C3′,5′-H), 7,12–7,26 (m, 2H, *C*2′,6′-H), 7,00–7,08 (m, 1H, C4′-H), 6,44–6,45 (s, 1H, C3-H), 6,42–6,43 (d, 1H, C-5). 13C NMR (125 MHz, DMSO-d_6, δ): 102,40; 108,74; 108,45; 115,50; 118,83; 128,55; 137,36; 154,78; 155,66; 157,94; 160,23; 163,57. IR (KBr, cm^{-1}): 3421 (NH), 3400, 3259, 3216 (OH, NH), 1629 (C═N), 1590 (C═C), 1231 (C—OH), 1134 (C—F), 1052 (N═C—S—C═N), 677 (C—S—C). Anal. Calcd for C14H10FN3O2S (303,32): C, 55,44; H, 3,22; N, 13,85. Found: C, 55,61; H, 3,23; N, 13,79.

2-(4-Fluorophenylamino)-5-(5-chloro-2,4-dihydroxyphenyl)-1,3,4-thiadiazole (FPCDT): Yield: 75%, mp: 241–243 °C. EI-MS (*m/z*, %): 337 (M+, 100), 303 (6), 187 (11), 168 (39), 154 (6), 141 (10), 136 (12), 128 (10), 110 (9), 95 (14), 83 (9), 69 (8), 63 (2), 51 (4). 1H NMR (500 MHz, DMSO-d_6, δ): 11,05 (s, 1H, *C*2-OH); 10,65 (s, 1H, C4-OH); 10,28 (s, 1H,

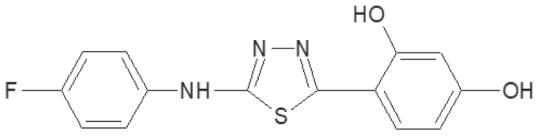

2-(4-Fluorophenylamino)-5-(2,4-dihydroxyphenyl)-1,3,4-thiadiazole (**FPDT**)

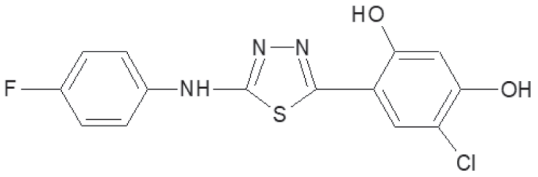

2-(4-Fluorophenylamino)-5-(5-chloro-2,4-dihydroxyphenyl)-1,3,4-thiadiazole (**FPCDT**)

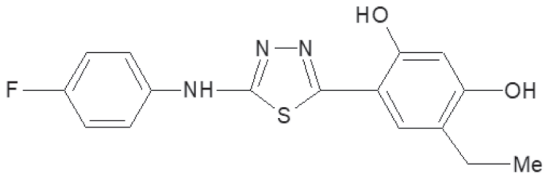

2-(4-Fluorophenylamino)-5-(5-ethyl-2,4-dihydroxyphenyl)-1,3,4-thiadiazole (**FPEDT**)

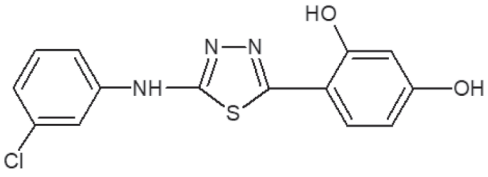

2-(3-Chlorophenylamino)-5-(2,4-dihydroxyphenyl)-1,3,4-thiadiazole (**CPDT**)

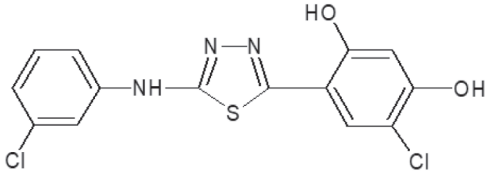

2-(3-Chlorophenylamino)-5-(5-chloro-2,4-dihydroxyphenyl)-1,3,4-thiadiazole (**CPCDT**)

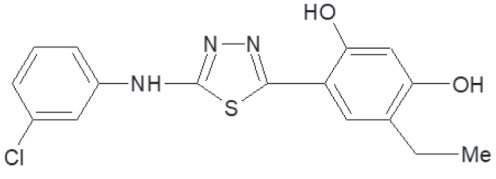

2-(3-Chlorophenylamino)-5-(5-ethyl-2,4-dihydroxyphenyl)-1,3,4-thiadiazole (**CPEDT**)

Fig. 2. Chemical structure of the 1,3,4-thiadiazole derivatives tested in this study.

NH); 7,93 (s, 1H, CAr-H); 7,67 (q, 2H, CAr-H); 7,19 (t, 2H, CAr-H); 6,68 (s, 1H, CAr-H). 13C NMR (125 MHz, DMSO-d_6, δ): 164,44; 158,08; 156,19; 155,29; 153,94; 152,75; 137,36; 127,37; 119,05; 115,66; 115,48; 111,65; 109,88; 103,73. IR (KBr, cm^{-1}): 3642 (NH), 3196 (OH), 3153 (NH), 2897 (CH), 2834 (CH), 1622 (C═N); 1566 (C═C), 1509 (C═C), 1484, 1447, 1391, 1295, 1260 (C—OH), 1219, 1189, 1158, 1105, 1052, 1011, 973, 866, 833, 811, 732. Anal. Calcd for C14H9N3O2SFCl (338,35): C, 49,90; H, 2,66; N, 12,41. Found: C, 49,81; H, 2,68; N, 12,47.

2-(4-Fluorophenylamino)-5-(5-ethyl-2,4-dihydroxyphenyl)-1,3,4-thiadiazole (FPEDT):

Yield: 73%, mp: 235–236 °C. EI-MS (EI, *m/z*, B): 331 (M+, 100), 316 (M-Me, 72), 181 (8), 168 (11), 148 (9), 110 (6), 95 (5), 69 (10), 65 (3). 1H NMR (500 MHz, DMSO-d_6, δ): 10,61 (s, 1H, *C*2-OH); 10,26 (s, 1H, C4-OH); 9,83 (s, 1H, NH); 7,67 (q, 3H, CAr-H); 7,19 (t, 2H, CAr-H); 6,55 (s, 1H, CAr-H); 2,51 (k, 2H, CH2Me); 1,14 (t, 3H, CH2Me). 13C NMR (125 MHz, DMSO-d_6, δ): 163,52; 158,02; 156,12; 155,11; 153,72; 137,41; 127,33; 122,52, 118,96; 115,62; 115,44; 107,87; 102,27; 20,07 (2C); 14,32 (3C). IR (KBr, cm^{-1}): 3379 (NH), 3257 (OH), 3212 (OH), 3165 (OH), 2959 (CH), 2832 (CH), 1625 (C═N); 1586 (C═C), 1510 (C═C), 1446, 1392, 1380, 1316, 1260, 1232 (C—OH), 1186, 1160, 1140, 1126, 1058, 1012, 973, 876, 824, 766, 744, 671. Anal. Calcd for C16H14N3O2SF (332,02): C, 58,12; H, 4,22; N, 12,65. Found: C, 58,03; H, 4,25; N, 12,73.

2-(3-Chlorophenylamino)-5-(2,4-dihydroxyphenyl)-1,3,4-thiadiazole (CPDT):

Yield: 77%, mp: 265–266 °C. EI-MS (*m/z*, %): 319 (M+, 100), 184 (36), 167 (5), 152 (5), 153 (10), 149 (16), 136 (8), 121 (5), 111 (6), 94 (10), 66 (5), 52 (3), 39 (4). 1H NMR (200 MHz, DMSO-d_6, δ): 9,80–11,02 (3H, *C*2,4-OH, NH), 7,92 (s, 1H, CAr-H), 7,81–7,84 (d, 1H, C6-H), 7,31–7,55 (m, 2H, CAr-H), 6,97–7,05 (m, 1H, CAr-H), 6,52 (s, 1H, C3-H), 6,42 (s, 1H, C5-H). 13C NMR (125 MHz, DMSO-d_6, δ): 102,42; 108,15; 108,43; 115,65; 116,57; 120,94; 128,50; 130,55; 133,44; 142,16; 155,09; 155,66; 160,40; 163,10. IR (KBr, cm^{-1}): 3245 (OH, NH), 1626 (C═N), 1598 (C═C), 1225 (C—OH), 1110 (C—Cl), 677 (C—S—C). Anal. Calcd for C14H10ClN3O2S (319,77): C, 52,59; H, 3,15; N, 13,14. Found: C, 52,39; H, 3,13; N, 13,19.

2-(3-Chlorophenylamino)-5-(5-chloro-2,4-dihydroxyphenyl)-1,3,4-thiadiazole (CPCDT):

Yield: 74%, mp: 264–266 °C. EI-MS (*m/z*, %): 353 (M+, 100), 319 (7), 200 (3), 186 (15), 184 (41), 169 (13), 149 (17), 128 (11), 111 (12), 100 (6), 90 (4), 75 (9), 69 (8), 63 (5), 51 (5). 1H NMR (500 MHz, DMSO-d_6, δ): 11,11 (s, 1H, *C*2-OH); 10,69 (s, 1H, C4-OH); 10,54 (s, 1H, NH); 7,96 (t, 2H, CAr-H); 7,48 (q, 1H, CAr-H); 7,38 (t, 1H, CAr-H); 7,04 (m, 1H, CAr-H); 6,71 (s, 1H, CAr-H). 13C NMR (125 MHz, DMSO-d_6, δ): 161,83; 155,37; 153,92; 153,08; 142,13; 133,43; 130,53; 127,22; 120,97; 116,62; 115,69; 111,61; 109,75; 101,67. IR (KBr, cm^{-1}): 3421 (NH), 3242 (OH), 3100 (OH), 2966 (CH), 2943 (CH), 2825 (CH), 1619 (C═N), 1599 (C═C), 1565 (C═C), 1510 (C═C), 1480, 1454, 1415, 1397, 1298 (C—OH), 1223, 1181, 1168, 1137, 1097, 992, 970, 925, 868, 845, 812, 771, 734, 721, 672, 615. Anal. Calcd for C14H9N3O2SCl2 (354,81): C, 47,59; H, 2,54; N, 11,84. Found: C, 47,68; H, 2,51; N, 11,89.

2-(3-Chlorophenylamino)-5-(5-ethyl-2,4-dihydroxyphenyl)-1,3,4-thiadiazole (CPEDT):

Yield: 78%, mp: 236–239 °C. EI-MS (*m/z*, %): 347 (M+, 100), 332 (M-Me, 84), 318 (3), 212 (3), 181 (12), 165 (10), 148 (14), 122 (6), 111 (8), 107 (6), 99 (3), 77 (6), 69 (15), 65 (5), 39 (4). 1H NMR (500 MHz, DMSO-d_6, δ): 10,64 (s, 1H, *C*2-OH); 10,43 (s, 1H, C4-OH); 9,84 (s, 1H, NH); 7,94 (d, 1H, CAr-H); 7,69 (s, 1H, CAr-H); 7,45 (q, 1H, CAr-H); 7,35 (t, 1H, CAr-H); 7,01 (q, 1H, CAr-H); 6,50 (s, 1H, CAr-H); 2,51 (k, 2H, CH2Me); 1,44 (t, 3H, CH2Me). 13C NMR (125 MHz, DMSO-d_6, δ): 163,01; 158,08; 155,46; 153,70; 142,23; 133,51; 130,53; 127,26; 122,55; 120,94; 116,63; 115,65; 107,92; 102,26; 22,08 (2C); 14,30 (3C). IR (KBr, cm^{-1}): 3367 (NH), 3252 (OH), 3187 (OH), 3126 (OH), 3058 (OH), 2961 (CH), 2829 (CH), 1621 (C═N), 1598 (C═N), 1555 (C═C), 1513 (C═C), 1482, 1453, 1390, 1318, 1278, 1261, 1225, 1187, 1136, 1094, 993, 926, 876, 819, 786, 771, 722, 671. Anal. Calcd for C16H14N3O2SCl (348,47): C, 55,37; H, 4,02; N, 12,05. Found: C, 55,47; H, 3,99; N, 12,11.

2.2. Reagents

The tested thiadiazole derivatives were dissolved in DMSO at a concentration of 5 mM. These working solutions were stored at room temperature (RT). TMZ was purchased from Sigma-Aldrich and a 100 mM working solution in dimethyl sulfoxide (DMSO) (Sigma-Aldrich) was prepared prior to storage at −20 °C. For all experiments, final concentration of DMSO was 0.1% (v/v). Minimum Essential Medium Eagle (MEME) was obtained from Sigma-Aldrich and Eagle's Minimum Essential Medium Eagle (EMEM) from ATCC. Dulbecco's Modified Eagle's Medium (DMEM), fetal bovine serum (FBS), fetal calf serum (FCS), non-essential amino acids penicillin and streptomycin were purchased from Gibco. Platelet-derived growth factor-BB (PDGF-BB) was purchased from Cell Signaling Technology. A 5 μg/ml working solution in 20 mM citrate, pH 3.0 was prepared prior to storage at −20 °C. Phosphate-buffered saline (PBS) and thiazolyl blue tetrazolium bromide (MTT) were obtained from Sigma-Aldrich.

2.3. Cell lines

Three human GBM cell lines were used in this study: T98G, U87MG and LN229. T98G cell line purchased from ATCC (CRL-1690™) was maintained in MEME supplemented with 50 U/mL penicillin, 50 μg/mL streptomycin, 1% non-essential amino acids and 10% FBS. U87MG cell line purchased from Sigma-Aldrich (89081402) was maintained in EMEM supplemented with 50 U/mL penicillin, 50 μg/mL streptomycin and 15% FBS. LN229 cell line (kindly provided by Rafał Krętowski, PhD, Department of Pharmaceutical Biochemistry, Medical University of Białystok, Poland) was maintained in DMEM supplemented with 50 U/mL penicillin, 50 μg/mL streptomycin, 10% FBS and glucose (4.5 g/l). Cells were routinely tested for mycoplasma contamination using Mycoplasma Detection Kit-Quick Test (Biotool). The used passage numbers were below 25. All cell lines were authenticated by ATCC using human short tandem repeat (STR) analysis. Normal human astrocytes (HA) were purchased from Lonza (CC-2565) and cultured in the AGM Astrocyte Growth Medium BulletKit containing Basal Medium supplemented with AGM SingleQuots Supplements according to the manufacturer's instruction. Cells were incubated at 37 °C, 5% CO_2 and 95% humidity.

2.4. Primary GBM culture

Clinical samples from patients with WHO grade IV GBM were collected from the Department of Neurosurgery and Pediatric Neurosurgery of the Medical University in Lublin, Poland. Prior written informed consent was obtained from patients, and the local Ethics Committee approved all procedures. Tumor samples were frozen vitally in freezing medium (FCS containing 10% DMSO) at −80 °C. Until unthawing, samples were kept at −80 °C for a maximum of 6 weeks. Patient-derived GBM cell lines were established according to the protocol by Mullins et al. [27]. Briefly, frozen tumor samples were thawed at 37 °C, minced by scalpels in DMEM/HAM's F12 medium supplemented with 10% FCS, 2 mM L-glutamine, penicillin-streptomycin and passed through cell strainer to obtain a single cell suspension. Cells were washed with PBS and seeded in 6-well plates coated with collagen. Outgrowing cells were detached with trypsin and expanded for subsequent analyses.

2.5. Cell viability assay

For the determination of cell viability, cells were seeded into 96-well plates at a density of 4×10^4 cells/well and incubated overnight at

37 °C. After this time, the cells were treated with the tested compounds or TMZ at serial concentrations for 48 h. Next, the medium was removed, the cells were washed with PBS and incubated in the culture medium with MTT solution at the final concentration of 0.5 mg/ml for 2 h at 37 °C. Then the medium was replaced with DMSO and absorbance was read at 570 nm using Elisa Bio-Rad Microplate Reader. Each compound in each concentration was tested in triplicate in a single experiment and five independent experiments were performed. On the basis of obtained results, the half maximal inhibitory concentration (IC_{50}) was calculated using the software GraphPad Prism 7.

2.6. Cell proliferation and colony formation assay

DNA synthesis as a marker for cellular proliferation was measured by bromodeoxyuridine (BrdU) incorporation using the colorimetric Cell Proliferation Elisa BrdU assay (Roche) according to the manufacturer's instruction. Briefly, cells (2x103 cells/well) were seeded in 96-well plates and incubated for 24 h. After this time, the culture medium was changed and the cells were treated with serial dilutions of FPDT or DMSO for 48 h. Next, BrdU was added for 2 h, and then cells were fixed for 30 min and incubated with BrdU antibody for 90 min. The absorbance values were measured at 415 nm using Elisa Bio-Rad Microplate Reader. Both FPDT in each concentration and DMSO was tested in triplicate in a single experiment and five independent experiments were performed.

To examine long-term toxicity of the tested compounds, a colony formation assay was performed. Cells were seeded in 6-well plates (100 cells/well). After 24 h the culture medium was changed and the cells were treated with serial dilutions of FPDT or DMSO for 2 weeks. Next, cell culture plates containing colonies were gently washed with PBS and fixed with 4% formaldehyde for 10 min. Wells were rinsed once again with PBS, colonies were stained with 0.5% crystal violet solution in 25% methanol for 10 min and the grossly visible colonies were counted. Four independent experiments were performed.

2.7. Cell migration assay

The cells were grown to confluence in 6-well plates grown to confluence. The cells were scratched using P200 pipette tip, washed with PBS and incubated in the serum free medium containing 25 μM FPDT or DMSO. The scratch was photographed under JuLI Smart Cell Analyzer and its width was measured at 0 and 24 h after scratching. Four independent experiments were performed.

2.8. Transwell chamber invasion assay

The invasion of GBM cells was evaluated using the transwell inserts with PET membrane (8 mm pore size) coated with matrigel (Corning) as a mimic of the extracellular matrix. After rehydration of the matrigel, 5×10^4 cells in medium with 0.5% FBS containing 25 μM FPDT or DMSO were seeded in the upper compartment of the insert. The lower compartment was filled with medium containing either 10% (for T98G and LN229 cells) or 15% FBS (for U87MG cells). Following 24-hour incubation, the upper surface of the membrane was wiped with a cotton swab to remove the remaining cells. Cells that invaded to the bottom side of the membrane were fixed with methanol and stained with 0.5% crystal violet solution in methanol. Membranes were placed on a glass slide, and three fields from each membrane were counted using an optical microscope. Three independent experiments were performed.

2.9. Protein isolation and western blot

Twenty-four hours after seeding, T98G cells were exposed either to DMSO or FPDT at IC_{50}. After 48 h of treatment, the cells were washed with PBS, harvested and sonicated in an ice cold lysis buffer (50 mM TRIS-HCl pH 8.0, 150 mM NaCl, 5 mM EDTA, 0.5% NP-40) supplemented with cocktails of protease and phosphatase inhibitors and sodium fluoride (Sigma-Aldrich). The lysates were centrifuged at 12,000*g* for 10 min at 4 °C and the protein concentration in the supernatants was determined using the BCA Protein Assay Kit (Pierce). Thirty μg of proteins were separated on 12% SDS-PAGE and transferred to nitrocellulose membranes. The membranes were blocked in 5% bovine serum albumin (BSA) in TBST (20 mM TRIS-HCl pH 7.5, 150 mM NaCl, 0.1% Tween 20) for 1 h at RT and next incubated with a primary antibody overnight at 4 °C. The following antibodies obtained from Cell Signaling (pAKT S473, #4060; AKT, #4691; pGSK3β S9, #5558; GSK3β, #9315) were used according to the manufacturer's instruction. After washing in TBST, the membranes were incubated with a secondary anti-rabbit antibody (Sigma-Aldrich) conjugated to horseradish peroxidase (HRP) for 1 h at RT. The blots were visualized on X-ray film using a SuperSignal West Pico Chemiluminescent Substrate (Pierce). Next, the membranes were stripped in 0.1 M glycine pH 2.9 and reused with a HRP-conjugated monoclonal antibody against glyceraldehyde 3-phosphate dehydrogenase (GAPDH) (Proteintech, #HRP-60004). The densitometric analysis was performed using G:Box system and GeneTools software (Syngene).

Table 1
Evaluation of the cytotoxic properties (mean $IC_{50} \pm$ SD [μM])[a] of the 1,3,4-thiadiazole derivatives in GBM cells and human astrocytes HA.

Compound	T98G[b]	U87MG[b]	LN229[b]	LUB04[c]	LUB07[c]	HA[d]
FPDT	53.53 ± 4.77	44.98 ± 9.71	55.20 ± 9.07	56.37 ± 7.18	67.73 ± 3.00	> 100
FPCDT	53.41 ± 4.94	48.21 ± 9.99	89.96 ± 8.64	62.84 ± 6.33	78.85 ± 7.33	97.27 ± 3.42
FPEDT	80.83 ± 9.85	50 ± 8.17	51.35 ± 14.28	58.43 ± 6.81	47.61 ± 7.85	27.22 ± 8.77
CPDT	48.16 ± 9.93	49.19 ± 9.73	63.15 ± 9.83	55.08 ± 9.84	73.22 ± 5.70	90.33 ± 9.30
CPCDT	30.78 ± 9.54	19.53 ± 9.03	35.60 ± 9.44	37.49 ± 5.09	34.89 ± 5.12	32.42 ± 8.37
CPEDT	28.75 ± 9.94	28.60 ± 4.92	30.00 ± 9.77	30.46 ± 2.39	38.76 ± 2.46	21.17 ± 6.53
TMZ	3426 ± 270	892 ± 37.20	978 ± 67.00	2826 ± 240	3597 ± 267	nd

nd - not determined.
[a] The concentration of compound that inhibit 50% of cell viability after 48 h of drug exposure measured by MTT assay.
[b] Human GBM cell line.
[c] Human patient-derived GBM cells.
[d] Human astrocytes.

2.10. Human phospho-kinase array

The human phospho-kinase array (R&D Systems, #ARY003) was performed according to the manufacturer's instructions, with a total protein amount of 400 μg per assay. Cells treated with DMSO and FPDT were handled and analyzed in parallel throughout the entire procedure. Exposure and data collection of each set of arrays was also performed in parallel. For data quantification, densitometric analysis of spots was performed using G:Box system and GeneTools software (Syngene). Intensity of the kinases' spots was normalized to the assay-internal positive controls after local background subtraction.

2.11. Statistical analysis

Western blot analysis and phospho-kinase array were performed three times. All other experiments were repeated at least four times. Results are reported as means and standard deviations. Statistical significance of comparisons was based on one-way ANOVA (multiple comparisons) or by paired *t*-test (comparison of two groups) in the software Graphpad Prism 7. Differences were considered statistically significant when $P < 0.05$.

3. Results and discussion

3.1. Influence of thiadiazole derivatives on cell viability

As mentioned in the Introduction section, previous studies revealed cytotoxic activity of FPDT and CPDT against several cancer cell lines including rat glioma C6 cell line [18,19], but their activity against human GBM cells has not been examined so far. Therefore, the primary aim of this study was to evaluate cytotoxicity of FPDT, CPDT, and their derivatives in GBM cells and commercially available HA. The IC_{50} (μM) values of the examined compounds and TMZ, the first-line chemotherapeutic for GBM, are listed in Table 1.

Our results clearly indicate that FPDT and CPDT inhibit viability of all three human GBM cell lines (T98G, U87MG and LN229) used in this study in a dose-dependent manner. These two compounds displayed a comparable cytotoxic activity against GBM cells ranging between 44.98 ± 9.71 μM and 55.20 ± 9.01 μM in case of FPDT or between 48.16 ± 9.93 μM and 63.15 ± 9.83 μM in case of CPDT. Cell lines do not fully recapitulate GBM heterogeneity which significantly contributes to therapeutic failure. Therefore, we have also tested the compounds' activity in the patient-derived GBM cells (LUB04 and LUB07) in which both FPDT and CPDT displayed considerable potency ranging from 56.37 ± 7.18 μM to 67.73 ± 3.00 μM and from 55.08 ± 9.84 μM to 73.22 ± 5.70 μM, respectively. Either of compounds appeared to be 18–70 times more potent than TMZ. It should be emphasized that FPDT presented $IC_{50} > 100$ μM for HA, suggesting its selective toxicity against GBM cells. CPDT appeared to be slightly toxic towards HA with IC_{50} value around 90 μM.

A growing body of evidence suggests that the hydrophobic substituent ($\pi > 0$) in the resorcinol ring of the compound may increase its potency against cancer cells [20–25]. Here we evaluated the cytotoxicity of derivatives of FPDT and CPDT containing either —Cl or $—CH_2CH_3$ substituent at C5-position of 2,4-dihydroxyphenyl. In case of compounds containing the chlorine substituent at C3-position of the phenyl group, our results confirmed the initial hypothesis that introduction of either chlorine or ethyl substituent at C5-position of the resorcinol ring leads to an increased activity of the 1,3,4-thiadiazole derivatives. CPCDT containing chlorine atom at C5-position of 2,4-dihydroxyphenyl showed increased cytotoxic activity against both GBM cells (IC_{50} between 19.53 ± 9.03 μM and 37.49 ± 5.09 μM). Similarly, the presence of the ethyl substituent resulted in enhancement of cytotoxicity as CPEDT displayed IC_{50} values between 28.60 ± 4.92 μM and 38.76 ± 2.46 μM on GBM cells. Of note, the IC_{50} values of each of CPCDT and CPEDT against GBM cells appeared to be 30–110 times lower compared to that of TMZ. However, this increased activity was also observed in HA (IC_{50} of 32.42 ± 8.37 μM and 21.17 ± 6.53 μM, respectively), disqualifying CPCDT and CPEDT from further studies.

In case of compounds containing the fluoro substituent at C4-position of the phenyl group, our initial hypothesis was not confirmed as neither chlorine, nor ethyl substituent at C5-position of the resorcinol ring significantly improved anti-GBM activity. FPCDT carrying chlorine atom at C5-position of 2,4-dihydroxyphenyl displayed IC_{50} from 48.21 ± 9.99 μM to 89.96 ± 9.77 μM towards GBM cells and 97.27 ± 3.42 μM towards HA. The presence of the ethyl substituent did not enhanced the anticancer activity as FPEDT showed IC_{50} values between 47.61 ± 7.85 μM and 80.83 ± 9.85 μM for GBM cells. However, such a modification markedly increased cytotoxicity against HA (IC_{50} of 27.22 ± 8.77 μM).

Based on current knowledge, it is impossible to point out the reasons of these findings. It has previously been postulated that the changes in the activity of 2-amino-1,3,4-thiadiazole derivatives may result from i). modifications of electronic properties important for interactions between compound and its molecular target; ii). effects of both intra- and inter-molecular hydrogen bonds [26]. Whether any of these elements influences the activity of derivatives examined in this study remains an open question.

Since FPDT exhibited anti-GBM activity ranging between 44.98 μM and 67.73 μM without affecting HA at 100 μM concentration, we subsequently selected this compound for further studies.

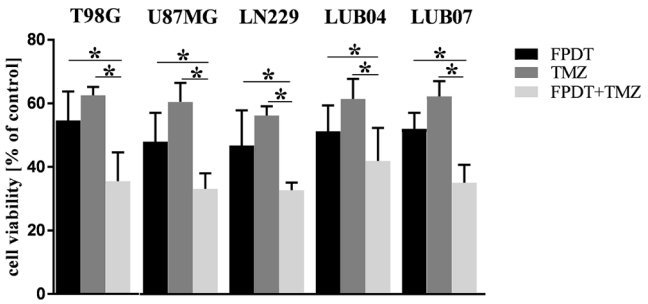

Fig. 3. Treatment with FPDT enhances an inhibitory effect of TMZ on viability of GBM cells. Graphs showing viability of cells treated with FPDT, TMZ or both agents after 48 h of continuous exposure at IC_{50}. Data are presented as mean ± SD (n = 5) expressed as percentage of control (DMSO-treated cells); *P < 0.05 (one-way ANOVA).

3.2. Effect of FPDT on TMZ activity in GBM cells

In order to determine whether FPDT can augment inhibitory effect of TMZ on cell viability, T98G, U87MG, LN229, LUB04 and LUB07 cells were incubated with FPDT, TMZ or both compounds at IC_{50}. Combined treatment with FPDT and TMZ resulted in enhanced inhibition of cell viability when compared to the single agent treatment (Fig. 3).

3.3. Influence of FPDT on proliferation of GBM cells

Previously, the effect of FPDT on tumor cells was attributed to decreased DNA synthesis [19,29]. Herein, we first measured the level of DNA synthesis by analysis of BrdU incorporation into DNA. In all three cell lines and patient-derived GBM cells exposed for 48 h to increasing concentrations of FPDT, a dose-dependent inhibition of BrdU incorporation was observed (Fig. 4A). Treatment with the highest, 100 μM, concentration of FPDT reduced DNA synthesis to 13, 13, 18, 9 or 14% respectively in T98G, U87MG, LN229, LUB04 or LUB07 cells as compared to the dimethyl sulfoxide (DMSO)-treated cells. We further investigated the antiproliferative effect of FPDT by colony forming assay. After 2 weeks of incubation under continuous drug exposure, a dose-dependent decrease of colony number was observed in all three cell lines and patient-derived cells (Fig. 4B). Treatment with 50 μM completely inhibited the ability of these cells to form colonies.

3.4. Influence of FPDT on migration and invasion of GBM cells

Diffuse infiltrative growth of GBM is one of the major factors in therapeutic failure, therefore new therapeutic strategies should inhibit not only proliferation, but also migration of GBM cells [28]. Here the effect of FPDT on ability of GBM cells to migrate was analyzed by a scratch assay. This analysis was conducted in T98G, U98MG and LN229 cell lines, as it was impossible to obtain a confluent monolayer of patient-derived GBM cells required to perform a scratch assay. In each cell line examined, markedly fewer cells treated for 24 h with 25 μM FPDT migrated into the scratched area compared to the control cells. Therefore, the width of the scratch gap in the FPDT-treated cells was significantly higher compared to the DMSO-treated cells (Fig. 5A, B). These results indicate that FPDT inhibits ability of T98G, U87MG and LN229 cells to migrate. We further assessed the influence of FPDT on invasive properties of GBM cells in Matrigel-coated Transwell inserts. In each cell line examined, significantly lower number of cells treated for 24 h with 25 μM FPDT invaded through the insert membranes compared to the DMSO-treated cells (Fig. 5C, D).

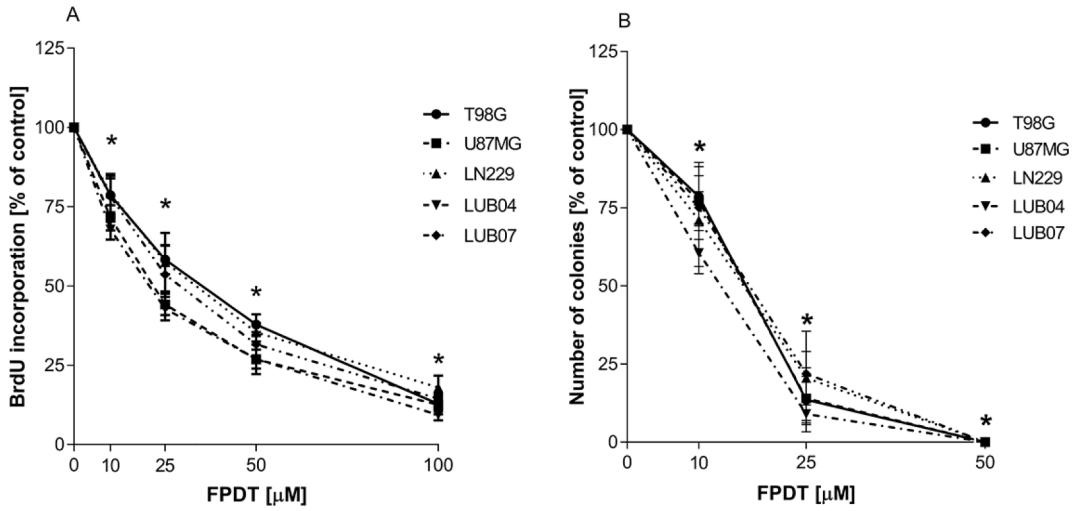

Fig. 4. FPDT decreases proliferation and ability to form colonies of GBM cells. **A** The cells were treated with serial dilutions of FPDT or DMSO for 48 h and next cell proliferation was assessed by BrdU assay. Data are presented as mean ± SD (n = 5) expressed as percentage of control (DMSO-treated cells); *P < 0.05 (one-way ANOVA). **B** The cells were treated with serial dilutions of FPDT or DMSO for 2 weeks and subsequently the colonies formed were fixed with paraformaldehyde, stained with crystal violet and counted. Data are presented as mean ± SD (n = 4) expressed as percentage of control (DMSO-treated cells); *P < 0.05 (one-way ANOVA).

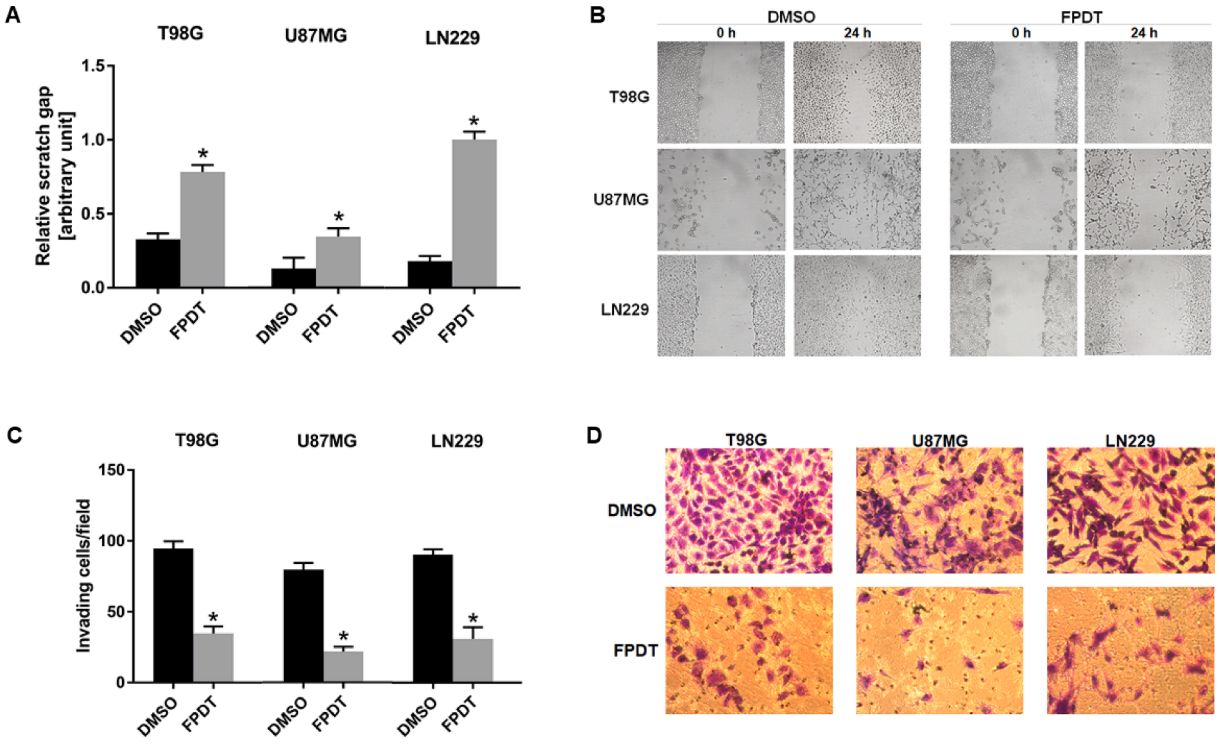

Fig. 5. Effect of FPDT on migration and invasion of GBM cells. The cells were scratch-wounded with a P200 tip and incubated in the serum free medium containing 25 μM FPDT or DMSO for 24 h. The width of the gap was measured at 0 and 24 h after scratching. **A** Relative scratch gap was calculated as the ratio of the remaining scratch gap at the given time point and the original gap at 0 h. Data are presented as mean ± SD (n = 4); *P < 0.05 (*t*-test). **B** Representative images of the scratch assay. **C** Quantitative analysis of cell invasion across Matrigel-coated Transwell inserts. Data are presented as mean ± SD (n = 3); *P < 0.05 (*t*-test). **D** Representative images of the invasion assay.

3.5. Effect of FPDT on the AKT pathway

Our previous study showed that FPDT inhibited phosphorylation of MEK, ERK, RSK90 kinases as well as CREB protein in non-small lung carcinoma cells [29]. Downregulation of several other kinase pathways, such as c-Met [10], FAK [30] or AKT [31], was observed in cancer cells treated with distinct 1,3,4-thiadiazole derivatives. Here we performed a phospho-kinase array in T98G cells to identify the molecules that could be potentially responsible for the antiproliferative and antimigratory effect of FPDT. This analysis showed a significant downregulation of p-GSK3α/β (S21/S9) and p-AKT (S473) in the cells treated with FPDT compared to the cells treated with DMSO (Fig. 6A, B). This down-regulation was confirmed by Western blot analysis (Fig. 6C, D). The level of total AKT and GSK3β remained unchanged upon FPDT treatment

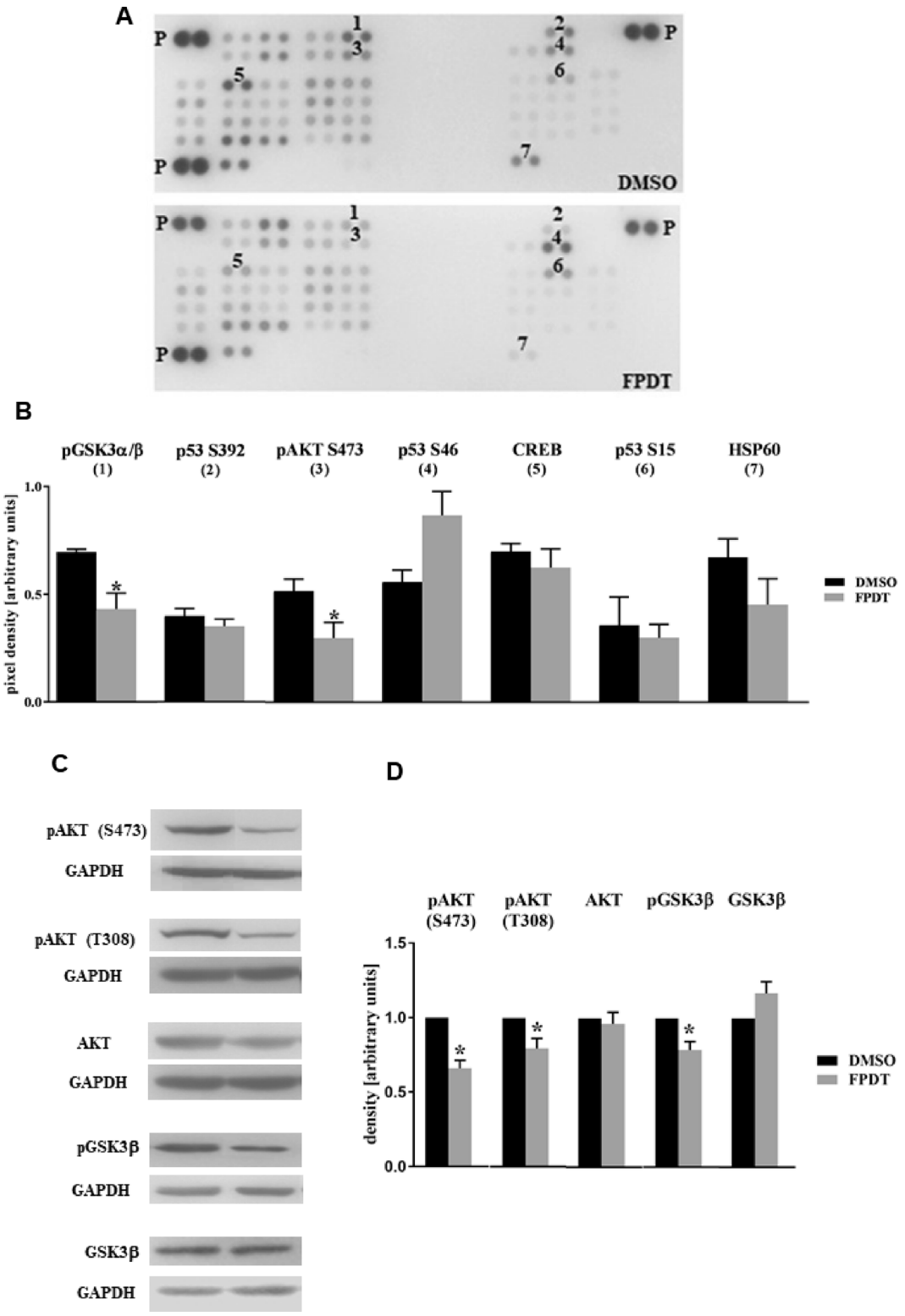

Fig. 6. Treatment with FPDT leads to downregulation of p-GSK3β and p-AKT which partially contributes to the diminished cell viability. **A** T98G cells were treated with DMSO or FPDT for 48 h prior to collecting the lysates. The lysates were incubated with the membranes of the human phospho-kinase array kit (R&D Systems) and bound phospho-proteins were detected according to the manufacturer's instructions. Each membrane contains antibody against particular kinase or positive control (P) spotted in duplicate. The membranes shown are representative for three independent experiments. **B** Densitometric analysis of spots 1 (p-GSK3α/β S21/S9), 2 (p-p53 S392), 3 (p-AKT S473), 4 (p-p53 S46), 5 (CREB), 6 (p-p53 S15) and 7 (HSP60) was performed using G:Box system and GeneTools software (Syngene). Each bar represents the mean ± SD of duplicate spots from three independent experiments; *P < 0.05 (*t*-test). **C** The level of selected proteins in T98G cells treated with DMSO or FPDT for 48 h was analyzed by Western blot. GAPDH was used as a loading control. **D** The graph shows quantification of protein bands intensity after normalization to GAPDH. Data are presented as mean ± SD (n = 3); *P < 0.05 vs DMSO (*t*-test).

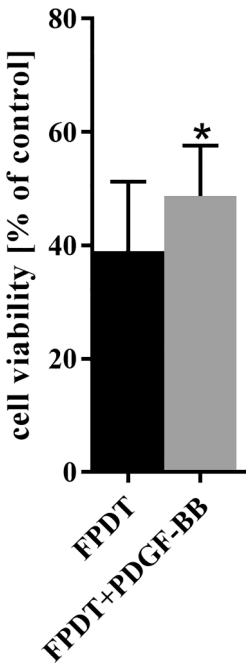

Fig. 7. The viability of T98G cells cultured in medium with or without PDGF-BB (50 ng/ml) for 24 h prior the exposure to FPDT at IC_{50} for 48 h. Data are presented as mean ± SD (n = 5); *P < 0.05 (*t*-test).

which implies that this compound decreases phosphorylation, but not expression of AKT and GSK3β.

As phosphorylation of GSK3β may be mediated by several kinases [32], its decreased phosphorylation upon FPDT treatment may not be a direct consequence of diminished AKT phosphorylation. The activity of AKT is tightly regulated at many levels in a context-dependent manner [33]. Therefore, further experimental work is needed in order to clarify the precise molecular mechanism underlying inhibition of AKT and GSK3β phosphorylation upon FPDT treatment.

Both AKT and GSK3β are involved in several cellular processes such as proliferation, cell cycle, growth, motility. Deregulated activity of each of these molecules as well as their targets, often observed in GBM, contributes to tumor growth and invasiveness. Hence, AKT and GSK3β signaling pathways constitute attractive targets for GBM therapy [34]. We therefore speculated that decreased phosphorylation of AKT and GSK3β observed in FPDT-treated cells might contribute to the reduced viability of these cells. Indeed, our results confirmed this hypothesis, as pretreatment with PDGF-BB, an activator of AKT phosphorylation [35], resulted in a significantly increased viability of FPDT-treated cells compared to the not pretreated with PDGF-BB counterparts (Fig. 7).

Our finding that FPDH influences the AKT/GSK3 β pathway in GBM, together with the previous notion that it modulates the ERK pathway in lung carcinoma cells [29], suggests that the direct molecular target of FPDT regulates action of several kinase-pathways, probably in a cell type-dependent manner. It is tempting to speculate that the mechanism underlying FPDT's activity is linked to some upstream signal molecules of the AKT and ERK pathways. For instance, several receptor tyrosine kinases (RTK) have been shown to activate RAS proteins, which in turn modulate both AKT and ERK pathways [36].

Aside from the question of the molecular target of FPDT, there is a question concerning its activity *in vivo*. Although discrepancy between the drug efficacy *in vitro* and *in vivo* is not a rule, it is relatively frequent phenomenon. In case of compounds that could serve as drugs against brain tumors, there is also a question about their ability to cross the BBB. The general assumption is that the molecule crosses the BBB if its molecular mass is less than 400–500 Da and it forms less than 8–10 hydrogen bonds with solvent water [37]. With a molecular mass of approximately 303 g/mol, FPDT seems to meet the first of these requirements. Further studies are necessary to conclude whether the second requirement is also fulfilled.

In summary, six 1,3,4-thiadiazole derivatives containing or not an additional —Cl or —CH_2CH_3 substituent at C5-position of 2,4-dihydroxyphenyl displayed anticancer activity in both human GBM cell lines and patient-derived GBM cells. The tested compounds presented the IC_{50} values 15–110 times lower compared to that of TMZ, the first-line chemotherapeutic agent for GBM. Introduction of either chlorine or ethyl substituent at C5-position of the resorcinol ring increased cytotoxicity of the 1,3,4-thiadiazole derivatives containing the chlorine substituent at C3-position of the phenyl group. Such a modifications did not improve anti-GBM activity of the 1,3,4-thiadiazole derivatives containing the fluoro substituent at C4-position of the phenyl group, but increased their toxicity to HA. FPDT appeared to be the most promising of the tested compounds, as it has shown IC_{50} values between 45 μM and 68 μM for GBM cells and >100 μM for HA. FPDT significantly augmented activity of TMZ and inhibited proliferation and ability to migrate of GBM cells. It also diminished phosphorylation level of GSK3β and AKT, which partially contributed to inhibition of cell viability. Our findings warrant further research on activity of FPDT against GBM.

Declaration of Competing Interest

The authors declare that they have no known competing financial interests or personal relationships that could have appeared to influence the work reported in this paper.

Acknowledgements

The authors wish to thank the patients for providing biological specimens for this study. We are grateful to Małgorzata Bogacińska-Karaś (MMRC PAS) for assistance in cell culturing. This work was financially supported by the National Science Centre of Poland, grant no: 2013/11/D/NZ7/00925 (to MS).

References

[1] M. Weller, T. Cloughesy, J.R. Perry, W. Wick, Standards of care for treatment of recurrent glioblastoma – are we there yet? Neuro Oncol. 15 (2013) 24–27, https://doi.org/10.1093/neuonc/nos273.
[2] D. Gramatzki, P. Roth, E.J. Rushing, J. Weller, N. Andratschke, S. Hofer, et al., Bevacizumab may improve quality of life, but not overall survival in glioblastoma: an epidemiological study, Ann. Oncol. 29 (2018) 1431–1436, https://doi.org/10.1093/annonc/mdy106.
[3] H.G. Wirsching, M. Weller, The Role of Molecular Diagnostics in the management of patients with gliomas, Curr. Treat. Options. Oncol. 17 (51) (2016), https://doi.org/10.1007/s11864-016-0430-4.
[4] S.A. Sprowls, T.A. Arsiwala, J.R. Bumgarner, N. Shah, S.S. Lateef, B.N. Kielkowski, et al., Improving CNS delivery to brain metastases by blood-tumor barrier disruption, Trends, Cancer. 5 (2019) 495–505, https://doi.org/10.1016/j.trecan.2019.06.003.
[5] S. Haider, M.S. Alam, H. Hamid, 1,3,4-Thiadiazoles: a potent multi targeted pharmacological scaffold, Eur. J. Med. Chem. 92 (2015) 156–177, https://doi.org/10.1016/j.ejmech.2014.12.035.
[6] S. Abu-Melha, M.M. Edrees, H.H. Salem, N.A. Kheder, S.M. Gomha, M.R. Abdelaziz, Synthesis and biological evaluation of some novel thiazole-based heterocycles as potential anticancer and antimicrobial agents, Molecules 24 (2019) 539, https://doi.org/10.3390/molecules24030539.
[7] S. Cascioferro, G.L. Petri, B. Parrino, D. Carbone, N. Funel, C. Bergonzini, et al., Imidazo[2,1-b] [1,3,4]thiadiazoles with antiproliferative activity against primary and gemcitabine-resistant pancreatic cancer cells, Eur. J. Med. Chem. 189 (2020), 112088, https://doi.org/10.1016/j.ejmech.2020.112088.
[8] K.M. Dawood, T.M. Eldebss, H.S. El-Zahabi, M.H. Yousef, P. Metz, Synthesis of some new pyrazole-based 1,3-thiazoles and 1,3,4-thiadiazoles as anticancer agents, Eur. J. Med. Chem. 70 (2013) 740–749, https://doi.org/10.1016/j.ejmech.2013.10.042. Epub 2013 Oct 30.
[9] D. Kumar, N. Maruthi Kumar, K.H. Chang, K. Shah, Synthesis and anticancer activity of 5-(3-indolyl)-1,3,4-thiadiazoles, Eur. J. Med. Chem. 45 (2010) 464–4668, https://doi.org/10.1016/j.ejmech.2010.07.023.
[10] L. Zhang, J. Zhao, B. Zhang, T. Lu, Y. Chen, Discovery of [1,2,4]triazolo[3,4-b] [1,3,4]thiadiazole derivatives as novel, potent and selective c-Met kinase inhibitors: Synthesis, SAR study, and biological activity, Eur. J. Med. Chem. 150 (2018) 809–816, https://doi.org/10.1016/j.ejmech.2018.03.049.

[11] Z. Chen, D. Li, N. Xu, J. Fang, Y. Yu, W. Hou, et al., Novel 1,3,4-selenadiazole-containing kidney-type glutaminase inhibitors showed improved cellular uptake and antitumor activity, J. Med. Chem. 62 (2019) 589–603, https://doi.org/10.1021/acs.jmedchem.8b01198.
[12] V. Raj, A.S. Bhadauria, A.K. Singh, U. Kumar, A. Rai, A.K. Keshari, et al., Novel 1,3,4-thiadiazoles inhibit colorectal cancer via blockade of IL-6/COX-2 mediated JAK2/STAT3 signals as evidenced through data-based mathematical modeling, Cytokine 118 (2019) 144–159, https://doi.org/10.1016/j.cyto.2018.03.026.
[13] S. Lindskog, Structure and mechanism of carbonic anhydrase, Pharmacol. Ther. 74 (1997) 1–20.
[14] K. Thangavelu, C.Q. Pan, T. Karlberg, G. Balaji, M. Uttamchandani, V. Suresh, et al., Structural basis for the allosteric inhibitory mechanism of human kidney-type glutaminase (KGA) and its regulation by Raf-Mek-Erk signaling in cancer cell metabolism, Proc. Natl. Acad. Sci. USA 109 (2012) 7705–7710, https://doi.org/10.1073/pnas.1116573109.
[15] L.A. McDermott, P. Iyer, L. Vernetti, S. Rimer, J. Sun, M. Boby, et al., Design and evaluation of novel glutaminase inhibitors, Bioorg. Med. Chem. 24 (2016) 1819–1839, https://doi.org/10.1016/j.bmc.2016.03.009.
[16] K. Shukla, D.V. Ferraris, A.G. Thomas, M. Stathis, B. Duvall, G. Delahanty, et al., Design, synthesis, and pharmacological evaluation of bis-2-(5-phenylacetamido-1,2,4-thiadiazol-2-yl)ethyl sulfide 3 (BPTES) analogs as glutaminase inhibitors, J. Med. Chem. 55 (2012) 10551–10563, https://doi.org/10.1021/jm301191p.
[17] M. El-Naggar, H.A. Sallam, S.S. Shaban, S.S. Abdel-Wahab, A.E.E. Amr, M.E. Azab, et al., Design, synthesis, and molecular docking study of novel heterocycles incorporating 1,3,4-thiadiazole moiety as potential antimicrobial and anticancer agents, Molecules 24 (2019) pii: E1066, https://doi.org/10.3390/molecules24061066.
[18] M. Juszczak, J. Matysiak, A. Niewiadomy, W. Rzeski, The activity of a new 2-amino-1,3,4-thiadiazole derivative 4ClABT in cancer and normal cells, Folia Histochem. Cytobiol. 49 (2011) 436–444.
[19] W. Rzeski, J. Matysiak, M. Kandefer-Szerszeń, Anticancer, neuroprotective activities and computational studies of 2-amino-1,3,4-thiadiazole based compound, Bioorg. Med. Chem. 15 (2007) 3201–3207.
[20] P.A. Brough, X. Barril, M. Beswick, B.W. Dymock, M.J. Drysdale, L. Wright, et al., 3-(5-Chloro-2,4-dihydroxyphenyl)-pyrazole-4-carboxamides as inhibitors of the Hsp90 molecular chaperone, Bioorg. Med. Chem. Lett. 15 (2005) 5197–5201.
[21] P.A. Brough, W. Aherne, X. Barril, J. Borgognoni, K. Boxall, J.E. Mansfield, et al., 4,5-diarylisoxazole Hsp90 chaperone inhibitors: potential therapeutic agents for the treatment of cancer, J. Med. Chem. 51 (2008) 196–218.
[22] S.Y. Sharp, K. Boxall, M. Rowlands, C. Prodromou, S.M. Roe, A. Maloney, et al., In vitro biological characterization of a novel, synthetic diaryl pyrazole resorcinol class of heat shock protein 90 inhibitors, Cancer Res 67 (2007) 2206–2216.
[23] M.M. Karpińka, J. Matysiak, A. Niewiadomy, Synthesis of novel 4-(1*H*-benzimidazol-2-yl)benzene-1,3-diols and their cytotoxic activity against human cancer cell lines, Arch. Pharm. Res. 34 (2011) 1639–1647.
[24] J. Matysiak, M.M. Karpińska, A. Niewiadomy, J. Wietrzyk, D. Kłopotowska, One-pot synthesis of new (1,3-thiazolo[5,4-b]pyridin-2-yl)benzenediols and their antiproliferative activities against human cancer cell lines, Chem. Biodivers. 9 (2012) 48–57.
[25] A. Niewiadomy, J. Matysiak, M.M. Karpińska, Synthesis and anticancer activity of new 2-aryl-4h-3,1-benzothiazines, Arch. Pharm. (Weinheim) 344 (2011) 224–230.
[26] J. Matysiak, A. Opolski, Synthesis and antiproliferative activity of N-substituted 2-amino-5-(2,4-dihydroxyphenyl)-1,3,4-thiadiazoles, Bioorg. Med. Chem. 14 (2006) 4483–4489.
[27] C.S. Mullins, B. Schneider, F. Stockhammer, M. Krohn, C.F. Classen, M. Linnebacher, Establishment and characterization of primary glioblastoma cell lines from fresh and frozen material: a detailed comparison, PLoS One. (2013) 8(8): e71070. doi: 10.1371/journal.pone.0071070. eCollection 2013.
[28] F. Lefranc, E. Le Rhun, R. Kiss, M. Weller, Glioblastoma quo vadis: Will migration and invasiveness reemerge as therapeutic targets? Cancer. Treat. Rev. 68 (2018) 145–154, https://doi.org/10.1016/j.ctrv.2018.06.017.
[29] M. Juszczak, J. Matysiak, M. Szeliga, P. Pożarowski, A. Niewiadomy, J. Albrecht, et al., 2-Amino-1,3,4-thiadiazole derivative (FABT) inhibits the extracellular signal-regulated kinase pathway and induces cell cycle arrest in human non-small lung carcinoma cells, Bioorg. Med. Chem. Lett. 22 (2012) 5466–5469, https://doi.org/10.1016/j.bmcl.2012.07.036.
[30] J. Sun, Y.S. Yang, W. Li, Y.B. Zhang, X.L. Wang, J.F. Tang, et al., Synthesis, biological evaluation and molecular docking studies of 1,3,4-thiadiazole derivatives containing 1,4-benzodioxan as potential antitumor agents, Bioorg. Med. Chem. Lett. 21 (2011) 6116–6121, https://doi.org/10.1016/j.bmcl.2011.08.039.
[31] J.Y. Chou, S.Y. Lai, S.L. Pan, G.M. Jow, J.W. Chern, J.H. Guh, Investigation of anticancer mechanism of thiadiazole-based compound in human non-small cell lung cancer A549 cells, Biochem. Pharmacol. 66 (2003) 15–24.
[32] E. Beurel, S.F. Grieco, R.S. Jope, Glycogen synthase kinase-3 (GSK3): regulation, actions, and diseases, Pharmacol. Ther. 148 (2015) 114–131, https://doi.org/10.1016/j.pharmthera.2014.11.016.
[33] J.R. Hart, P.K. Vogt, Phosphorylation of AKT: a mutational analysis, Oncotarget 2 (2011) 467–476, https://doi.org/10.18632/oncotarget.293.
[34] E. Majewska, M. Szeliga, AKT/GSK3β Signaling in Glioblastoma, Neurochem. Res. 42 (2017) 918–924, https://doi.org/10.1007/s11064-016-2044-4.
[35] B.H. Rauch, A. Weber, M. Braun, N. Zimmermann, K. Schrör, PDGF-induced Akt phosphorylation does not activate NF-kappa B in human vascular smooth muscle cells and fibroblasts, FEBS Lett. 481 (2000) 3–7.
[36] D.K. Simanshu, D.V. Nissley, F. McCormick, RAS proteins and their regulators in human disease, Cell 170 (2017) 17–33, https://doi.org/10.1016/j.cell.2017.06.009.
[37] W.M. Pardridge, The blood-brain barrier: bottleneck in brain drug development, NeuroRx 2 (2005) 3–14, https://doi.org/10.1602/neurorx.2.1.3.